AUT Journal of Mechanical Engineering

AUT J. Mech. Eng., 1(1) (2017) 13-20
DOI: 10.22060/mej.2016.762

Numerical Investigation of Nano Particles Dispersion and Deposition in Fully Developed Laminar Pipe Flows

P. Talebizadeh[1], H. Rahimzadeh[1*], G. Ahmadi[2], R. Brown[3], K. Inthavong[4]

[1] Department of Mechanical Engineering, Amirkabir University of Technology, Tehran, Iran
[2] Department of Mechanical and Aeronautical Engineering, Clarkson University, New York, USA
[3] Biofuel Engine Research, Queensland University of Technology, Brisbane, Australia
[4] School of Aerospace, Mechanical and Manufacturing, Engineering, RMIT University, Melbourne, Australia

ABSTRACT: The aim of this paper is to study the deposition and dispersion of nano particles in fully developed laminar pipe flows numerically. To simulate particle transport and to locate the position of particles, the Eulerian - Lagrangian method is used under the conditions of one-way coupling. Due to studied range of particle diameters from 5 nm to 100 nm, the main effective force for particle deposition is the Brownian diffusion force. After studying the mesh independency and validating results, time history analysis of particle transport is also performed by injecting the particles from the inlet surface and tracking them at each moment. Furthermore, the effective parameters, i.e. particle diameter, pipe length and diameter, temperature and particle density are studied comprehensively. The results of time history analysis of particle transport show that nano particles with less diameters are more deposited in less time. Furthermore, maximum number of escaped particles from the pipe occurred at 0.035 s after injecting the particles for all studied particle diameters due to the studied flow rate and length of the pipe. The output of this study can provide a guideline for evaluating nano particle transport and deposition in fully developed laminar pipe flows.

Review History:
Received: 9 November 2015
Revised: 14 February 2016
Accepted: 9 May 2016
Available Online: 9 November 2016

Keywords:
Two phase gas – solid flow
Nano particles
Particle deposition
Fully developed laminar flow
Lagrangian particle tracking

1- Introduction

Dispersion and deposition of aerosol particles have attracted attention of many researchers due to their wide applications in medical, environmental, and industrial fields [1]. Particle separator devices, particle released from combustion and aftertreatment systems, drug delivery and particle deposition in human respiratory tract are some applications of particle transport study. Moreover, the negative effect of particles especially nano particles on human health and the environment as well as more stringent exhaust emission regulations in recent years are the other reasons to show the importance of this phenomenon more than before [1-4].

Nano particle deposition in tubular pipe flows has lots of application and has been investigated earlier in the literature. A few studies have developed theoretical and empirical expressions for particle deposition in smooth tubes for developing and fully developed flows due to their Brownian diffusion [5, 6]. Thomas [7] developed a mathematical model for particle deposition in a wide range of particle diameters. Ingham [5, 8, 9] presented different models for particle deposition for plug, Poiseuille and combination of plug and Poiseuille flows. Yeh and Schum [10] presented a model for particle deposition in fully developed tubular flows. The presented model is a little different with the Ingham equation. Cohen and Asgharian [6] developed a model for particle deposition with the diameters higher than 10 nm in fully developed turbulent flows. Most of these studies have used the mass convection-diffusion equation for concentration of particles and developed analytical correlations for the deposition efficiency.

In addition to the analytical approaches, there are a number of studies in the literature that employed the Eulerian-Lagrangian particle tracking method to evaluate the deposition efficiency of nano-particles. Original model for the Lagrangian Brownian simulation model was introduced by Li and Ahmadi [11, 12] and also Ounis et al. [13]. Zamankhah et al. [14] studied particle deposition in a tubular pipe in order to validate the results of particle deposition in the nasal cavity and oral air path. Inthavong et al. [15] studied the deposition of particles in nasal cavity and trachea. They simulated particle deposition in fully developed tubular pipe flows for different particle diameters and Reynolds numbers using the FLUENT software. They developed a User Defined Function (UDF) to simulate the Brownian motion in the FLUENT software. Longest and Vinchurkar [16] investigated particle transport in oral air path using the Lagrangian particle tracking method. They simulated particle deposition in both fully developed and developing tubular pipe flows and compared the results with the Eulerian method. They showed that the Lagrangian method due to considering the inertia effect as well as all the effective forces in particle equation of motion is more effective than the Eulerian method. Krause et al [17] numerically and experimentally studied nano particle deposition in mouth cavity for both laminar and turbulent flows. They studied particle deposition in a tubular pipe and a bend for their code validation. Shi et al. [18] also studied two-phase flows in oral air path and used a tubular pipe for their

Corresponding author, E-mail: rahimzad@aut.ac.ir

code verification. Yin and Dai [19] experimentally studied particle deposition in horizontal pipes and compared their results with the existing empirical equations. They showed that particle deposition efficiency decreases by increasing the Reynolds number. There are more papers in the literature that studied particle deposition in tubular pipes [20-26]

Most of the previous studies have studied the transport of nano particles in pipes and compared them with the exact solutions in order to verify their codes [14]. Therefore, in this study, a comprehensive investigation on deposition and dispersion of nano particles in tubular pipes is performed using the Lagrangian particle tracking method. Furthermore, different effective parameters, i.e. length and diameter of the pipe, nano particle diameter, temperature and particle density on the deposition of nano particles are studied. Furthermore, time history analysis of particle transport is studied. It should be mentioned that the results of this study have a complementary role for the previous studies and the novelty of the paper is studying the time history analysis of particle transport, not presented in previous papers.

2- Mathematical modeling

In the following, first, governing equations of flow feild and nano particles are discussed. Then, the geometry, as well as the boundary conditions are presented.

2- 1- Fluid flow and particle governing equations

For an incompressible, steady and three-dimensional air flow, governing equations are the well-established conservations of mass and momentum. Due to low concentration of nano particles in the flow field, effect of particles on the flow is negligible. Therefore, the governing continuity and momentum equations for the fluid flow are given as:

$$\frac{\partial}{\partial t}(\rho\phi)+div(\rho\vec{V}\phi-\Gamma_{\phi}\,grad\,\phi)=S_{\phi} \quad (1)$$

where ρ is the fluid density, φ is the dependence variable, $\vec{V}$ is the velocity vector, Γ_{φ} is the conversion coefficient and S_{φ} is the source term.

In the Lagrangian study of particles, by employing the Newton' law for a particle with a mass of m, the particle equation of motion is given as [27]:

$$m\frac{du^{p}}{dt}=\sum F \quad (2)$$

In the above equation, F can be each applied force on the particle such as drag, lift, thermophoresis, gravity or the Brownian. For nano particles due to considering a diluted flow and also constant temperature throughout the pipe, the particle equation of motion including the drag and Brownian forces is given as:

$$\frac{du_i^{p}}{dt}=\frac{3\pi\mu(u_i^{f}-u_i^{p})}{C_c}d_p(1+0.15\,\mathrm{Re}_p^{0.687})+F_{Brownian} \quad (3)$$

The first term in the above equation is related to the Drag force for a Reynolds number below 1000, where u_i^{p} and u_i^{g} are the components of the particle and local fluid velocity, respectively. μ is the fluid viscosity and ρ_p is the particle density. Here C_c is the Cunningham correction factor to the Stokes drag law defined as [11, 12]:

$$C_c=1+\frac{2\lambda}{d_p}(1.257+0.4e^{-1.1d_p/2\lambda}) \quad (4)$$

where is the mean free path of air which is equal to 65 nm [27]. The amplitude of the Brownian force is given as [11]:

$$F_{Brownian}=\zeta\sqrt{\frac{\pi S_0}{\Delta t}} \quad (5)$$

where ζ is a zero-mean, unit-variance independent Gaussian random number, Δt is the time step for particle integration and S_0 is the spectral intensity function defined as [11]:

$$S_0=\frac{216\nu k_B T}{\pi^2\rho_g d_p^5\left(\frac{\rho_p}{\rho_g}\right)^2 C_c} \quad (6)$$

In the above equation, T is the absolute temperature of the fluid, ν is the kinematic viscosity, k_B is the Boltzmann constant and ρ_g is the gas density.

2- 1- The geometry

The studied geometry in this paper is a tubular pipe, which is shown in Fig. 1. Different diameters of 2.25, 4.5 and 9 mm and pipe lengths of 1 to 6 cm are studied.

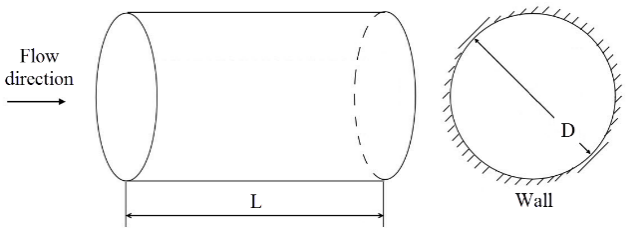

Fig. 1. A schematic view of the studied geometry

Computational mesh is generated by using ICEM CFD, which is presented in Fig. 2. The illustrated mesh consists of 2013165 hexahedral cells with an -increased mesh density near the wall for handling near-wall particle deposition correctly.

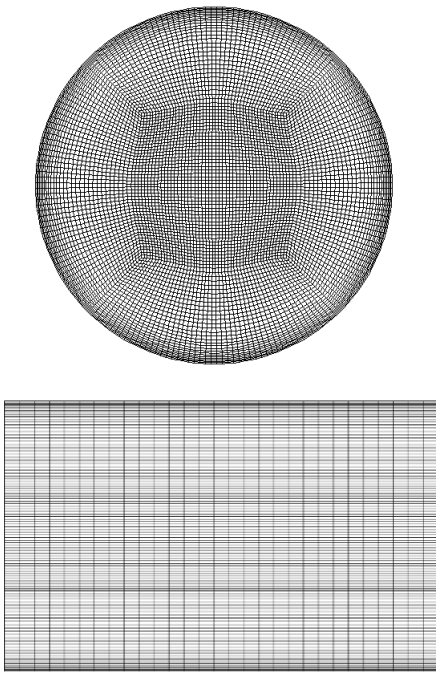

Fig. 2. Computational mesh at different cross sections of the pipe

2- 3- Boundary conditions

To have a fully developed flow, the exact solutions for laminar velocity profiles were imposed at the pipe inlet. Then, the flow was driven by solving the governing continuity and momentum equations in a 3D domain. The parabolic velocity profile for the fully developed laminar tubular flow is given as:

$$u(r) = 2u_{av}(1 - \frac{r^2}{R^2}) \quad (7)$$

where R is the pipe radius and u_{av} is the average velocity. Furthermore, the outflow condition is used for the outlet surface and no-slip condition is used for the walls.

Spherical particles were released uniformly at a distance of 2 mm from the inlet in the flow field to prevent any spurious data due to particles exiting the inlet upon immediate release. A separate code is prepared in the MATLAB software to find the locations of the particles, which is then imported into the FLUENT software.

In order to account for the variation of velocity on the flux of the particles, the fully developed inlet profile given by Eq. (7) is used for the tubular pipe. Then, the deposition efficiency is calculated based on the ratio of mass deposition rate to the inlet mass flow rate as:

$$DE = \frac{\dot{m}_w}{\dot{m}_{in}} \quad (8)$$

Note that 70000 particles are considered for the simulations [28, 29]. Furthermore, in the FLUENT software, particles are deposited when they hit the walls and then exit from the solution domain. This is corrected due to the considered range of studied particles [27].

As mentioned, the ANSYS Fluent® code was used to solve the governing equations of motion. A second order discretization was used with the pressure–velocity coupling resolved through the SIMPLE method.

3- Results and discussion

As mentioned, the fully developed tubular flow profile at the inlet is used to reach a fully developed flow throughout the entire pipe. In other words, the Navier-Stokes equations are solved with a fully developed boundary condition. Fig. 3 shows variation of the velocity at three cross sections of the pipe. As shown, the velocity is completely fully developed in the entire domain.

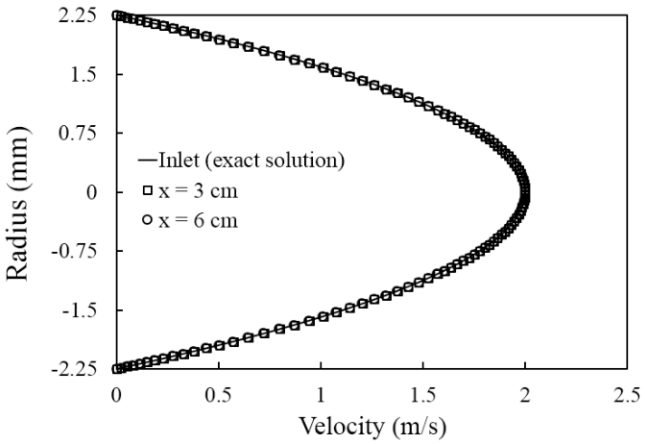

Fig. 3. Comparison of velocity profile at different cross sections of the pipe

Before studying the effect of different parameters and validation of the code, the mesh independency analysis is performed. In Table 1, cell numbers as well as particles deposition efficiency for 10 nm particles, a pipe with diameter of 4.5 mm and length of 6 cm are presented. As shown, the results of the three studied computational grids are close to each other due to considering a similar dense mesh at the near-wall region for all the computational meshes. At last, since deposition efficiency is highly close for the second and third grids, we chose the second mesh for the following studies.

Table 1. Mesh independency analysis for 10 nm particles in a pipe with a diameter of 4.5 mm and length of 6 cm

Mesh number	Cell numbers	Deposition efficiency (%)
1	780615	1.82
2	2013165	1.89
3	3812405	1.91

Validity of the present study is examined by comparing the simulation results for particle deposition efficiency in tubular pipes with the existing analytical correlations in the literature. These correlations were developed based on the dimensionless diffusion parameter Δ for fully developed laminar pipe flows with the parabolic velocity profile at the inlet. One of the frequently used correlations was developed by Ingham [5] which is given as:

$$DE = 1 - (0.819e^{-14.63\Delta} + 0.0976e^{-89.22\Delta} + 0.0325e^{-228\Delta} + 0.0509e^{-125.9\Delta^{2/3}}) \quad (9)$$

where

$$\Delta = \frac{\tilde{D}L_{pipe}}{U_{in}d^2} \quad (10)$$

and L_{pipe} is the pipe length, U_{in} is the average inlet velocity and d is the pipe diameter. $\tilde{D}$ is the diffusion coefficient which is determined as Eq. (11) [11].

$$\tilde{D} = \frac{k_b T C_c}{3\pi\mu d_p} \quad (11)$$

Fig. 4 displays the simulated deposition efficiency of 5 nm to 100 nm particles for a tubular pipe with a diameter of 4.5 mm and different lengths. Here the inlet fluid velocity is 1 m/s. It is seen the simulation results show excellent agreement with the empirical equation of Ingham [5]. Note that the Ingham equation [5] is obtained by solving the mass equation at the steady condition for fully developed tubular pipes.

Most of the previous studies compare their results with Ingham equation [5]. However, there are more equations in the literature to calculate the deposition efficiency by the Brownian diffusion in fully developed tubular pipes. Yeh and Schum [10] presented the deposition efficiency as:

$$DE = 1 - (0.819e^{-14.63\Delta} + 0.0976e^{-89.22\Delta} + 0.0325e^{-228\Delta} + 0.0509e^{-158.6\Delta^{2/3}}) \quad (12)$$

Gormley and Kennedy [30] also developed an equation for DE as:

$$DE = 6.61\Delta^{2/3} - 4.8\Delta - 1.123\Delta^{4/3} \quad (13)$$

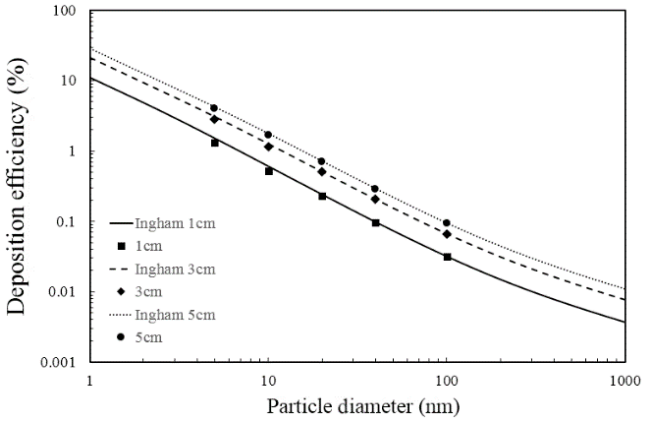

Fig. 4. Deposition efficiency versus particle diameter for fully developed tubular flow for various pipe lengths for an inlet fluid velocity of 1 m/s and pipe diameter of 4.5 mm

Fig. 5 displays the simulated deposition efficiency for a tubular pipe with a diameter of 4.5 mm and length of 4 cm. Here the inlet fluid velocity is 1 m/s. In this figure, all the mentioned equations are used for validating the present study. It is seen that the simulation results show a good agreement with different empirical equations.

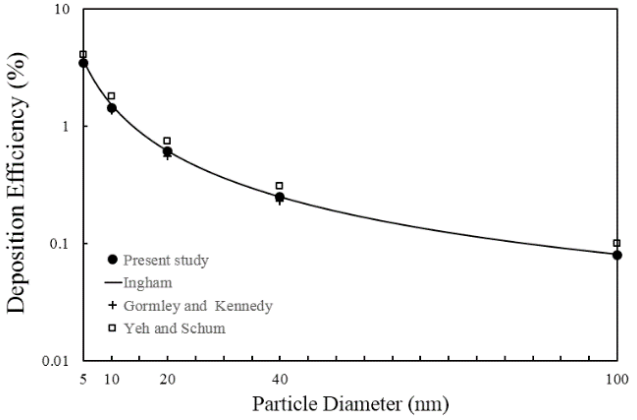

Fig. 5. Deposition efficiency versus particle diameter for fully developed tubular flow compared to different empirical equations for an inlet fluid velocity of 1 m/s and pipe diameter of 4.5 mm

Note that in Fig. 4, both axes are displayed in Logarithmic scale. However, in Fig. 5, only the y axis is shown in Logarithmic scale.

3- 1- Effect of different parameters on deposition of nano particles in tubular pipes at steady condition

3- 1- 1- Effect of pipe diameter

Fig. 6, below, displays the determined deposition efficiency for different particle diameters for a pipe with a length of 5 cm and various diameters. As shown, *DE* increases by decreasing the particle diameter due to the stronger Brownian force for smaller particles. Furthermore, by decreasing the pipe diameter, for a constant mean velocity and a constant number of injected particles, *DE* increases due to the higher area of the wall.

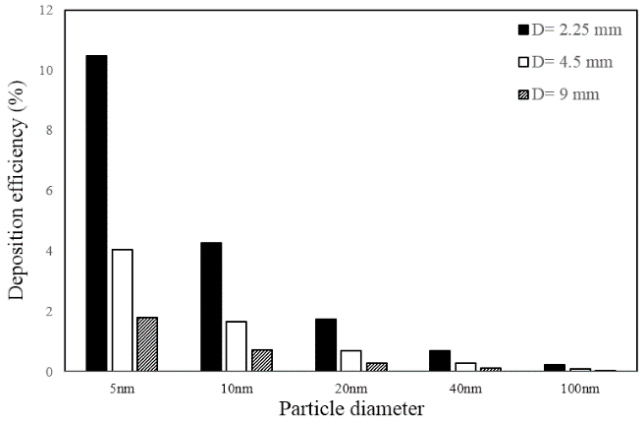

Fig. 6. The effect of pipe diameter on deposition efficiency of various particle diameters for fully developed tubular flow with an inlet mean velocity of 1 m/s and a pipe length of 5 cm

3- 1- 2- Effect of inlet velocity

Fig. 7 displays the determined deposition efficiency for various mean fluid velocities for different particle diameters. As shown, *DE* increases by decreasing the fluid velocity. Because, by increasing the velocity, the gas residence time in the pipe decreases and therefore the particles have less time to deposit on the wall.

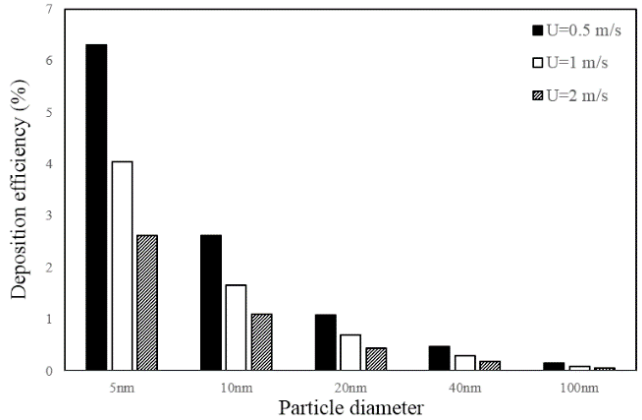

Fig. 7. The effect of fluid velocity on deposition efficiency of various particle diameters for fully developed tubular flow for a pipe diameter of 4.5 mm and a pipe length of 5 cm

3- 1- 3- Effect of pipe length

Fig. 8, shows the effect of pipe length on particle deposition efficiency. As expected, by increasing the pipe length, higher number of particles are deposited on the pipe walls and therefore higher *DE* can be achieved. However, the increase rate of *DE* decreases by increasing the pipe length. For example, for 5 nm particles, *DE* is equal to 1.31% and 2.13% in 1 cm and 2 cm pipes, respectively. Therefore, in the first 1 cm of the pipe, more particles are deposited on the walls.

3- 1- 4- Effect of temperature

When the temperature changes, the fluid properties and intensity of the Brownian force are altered. Therefore, the deposition efficiency also changes. Increasing the temperature, increases the diffusion coefficient, which results in a higher random movement of nano, particles, and

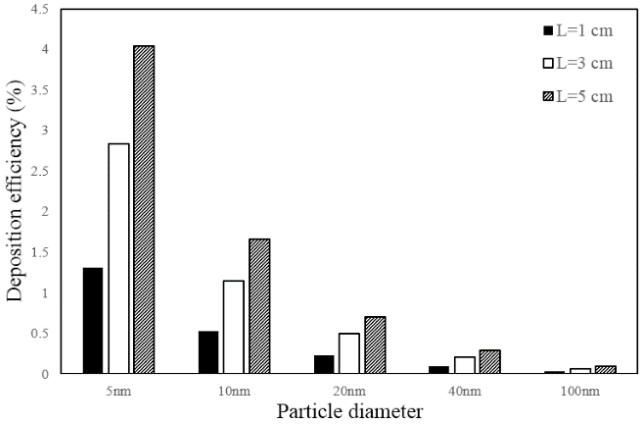

Fig. 8. The effect of pipe length on deposition efficiency of various particle diameters for fully developed tubular flow for a pipe diameter of 4.5 mm and inlet velocity of 1 m/s

therefore, increases the Brownian force. On the other hand, it increases the viscosity of the fluid, which decreases the diffusion coefficient of the particles, and therefore decreases the Brownian force. Fig. 9, displays the effect of temperature on particle deposition efficiency for a pipe with the length of 5 cm and diameter of 4.5 mm with an inlet velocity of 1 m/s. As shown, by increasing the temperature of the fluid and particles, deposition efficiency increases for all particle diameters. Therefore, the effect of higher collisions of the particles due to increasing the temperature is more pronounced than a higher viscosity of the air.

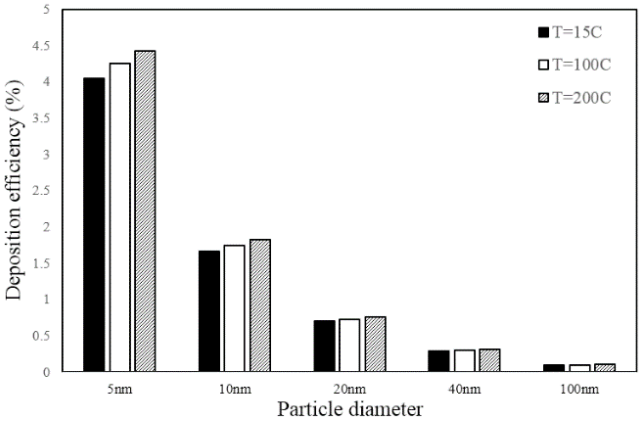

Fig. 9. The effect of temperature on deposition efficiency for various particle diameters for fully developed tubular flow for a pipe diameter of 4.5 mm, pipe length of 5 cm with the inlet velocity of 1m/s

To gain a better understanding of the effect of temperature, Fig. 10 displays the deposition efficiency for different particle diameters with constant properties of the fluid at 15 °C for the mentioned pipe. As shown, increasing the temperature alone has a considerable effect on the particles deposition efficiency.

As shown in Figs. 9 and 10, increasing the temperature has the highest effect on 5 nm particles and by increasing the particle diameter, this effect is reduced, so that for 100 nm particles, the temperature has a negligible effect on *DE*. The reason is due to the increase in the Brownian force by decreasing the particles diameter. In other words, the Brownian force is increased equally for all the particles diameters by

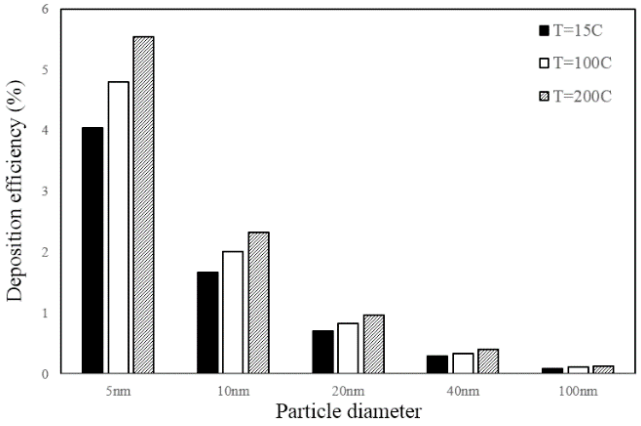

Fig. 10. The effect of temperature on deposition efficiency of various particle diameters considering constant viscosity of air for fully developed tubular flow with a pipe diameter of 4.5 mm, pipe length of 5 cm and the inlet velocity of 1 m/s

increasing the temperature. However, due to higher effect of the Brownian force on smaller particles, this increase in the Brownian force shows a higher impact on smaller particles.

3- 1- 5- Effect of particle density

Fig.11 shows the effect of particles density on *DE* in a pipe with 4.5 mm diameter and 5 cm length. The inlet velocity is equal to 1 m/s. As shown, due to the dominance of the Brownian diffusion mechanism on particles deposition and less relation of nano particles to density due to their size, changing the density has a negligible effect on the *DE*. Moreover, due to the random characteristics of the Brownian force, the results for each diameter are a little different [3]. It can be shown that from Ingham equation, the deposition efficiency is not a function of particle density [5].

3- 2- Time history analyses of particle transport and deposition in a fully developed pipe flow

For a pipe with a length of 6 cm and diameter of 4.5 mm, time histories of particles transport and deposition are evaluated for different nano particle diameters. In the simulations, the mean airflow velocity is 1 m/s. The particles were uniformly injected and at one time, from the injection surface and then the number of deposited and escaped particles are determined

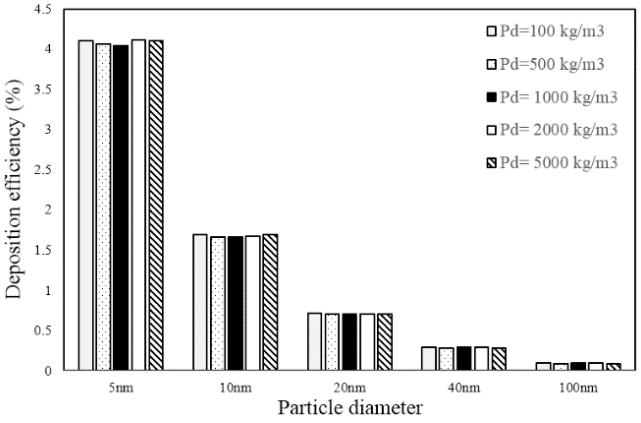

Fig. 11. The effect of particle density on deposition efficiency for various particle diameters for fully developed tubular flow for a pipe diameter of 4.5 mm, pipe length of 5 cm and the inlet velocity of 1m/s

at different periods. Therefore, the residence time of particles with different diameters can be determined.

Fig. 12a shows number of deposited, escaped, suspended inside particles as well as the total number of simulated particles at each moment for 5 nm particles. Fig. 12b shows total number of deposited and escaped particles through the time for 5 nm particles. Note that the total number of deposited particles at time t is equal to the sum of number of deposited particles from the beginning to time t. The number of deposited and escaped particles was evaluated from the simulation at every $\Delta t = 0.005$ s. It means that at every 0.005 s, the number of deposited or escaped particles are evaluated. It should be noted that the time interval should be small enough to show perfectly any changes in the particle number. The results show that at 0.32 s after the particle injection, all particles leave the domain, and almost 17.5% of the particles are deposited on the walls and the rest escape from the outlet. The maximum number of escaped particles over $\Delta t = 0.005$ s occurs at 0.035 s after the injection. Furthermore, after 0.2 s from the injection, majority of particles leave the domain and just a few particles remain at the domain. As shown in Fig. 12b, after this time, the total number of deposited and escaped particles almost remains constant. Figs. 13a and 13b are presented for 40 nm particles.

The variation of deposited and escaped particles for 40 nm particles is similar to 5 nm particles. The difference is in the number of deposited particles and the time duration that all particles leave the domain.

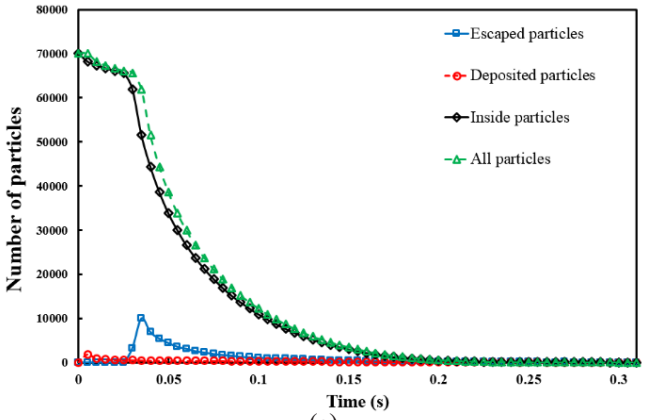

(a)

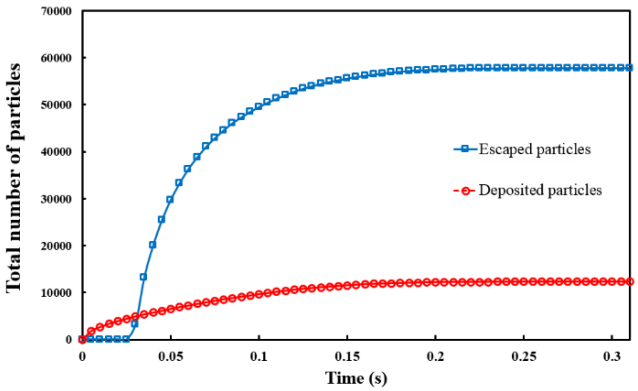

(b)

Fig. 12. The variation of (a) number of deposited, escaped, inside as well as all particles and (b) total number of deposited and escaped particles at each moment for 5 nm particles

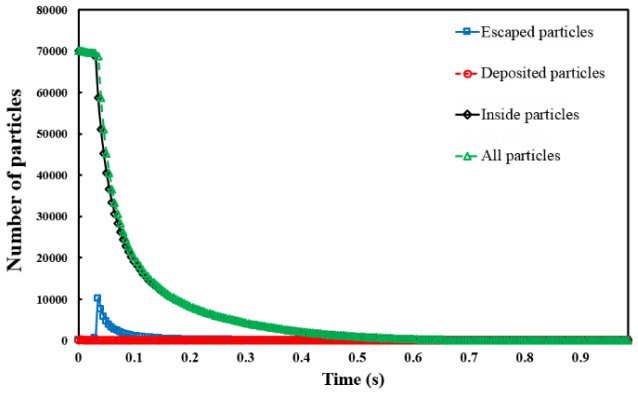

(a)

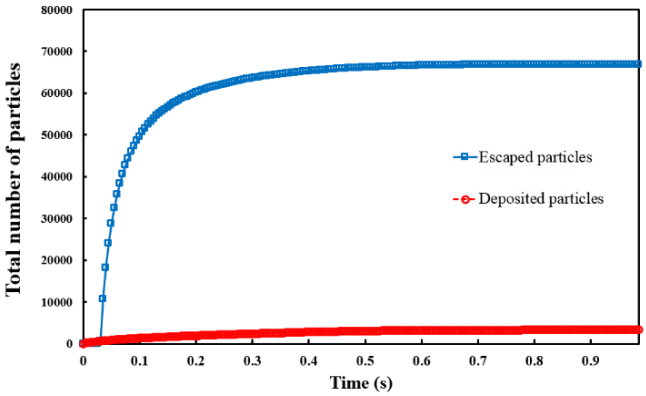

(b)

Fig. 13. The variation of (a) number of deposited, escaped, inside as well as all particles and (b) total number of deposited and escaped particles at each moment for 40 nm particles

Fig. 14a shows the total number of deposited particles as a function of time for all the studied diameters. As shown, for smaller particles, higher number of particles are deposited in a shorter time. In Fig. 14b, the variation of the total number of escaped particles is shown for all particle diameters. As also shown, smaller particles leave the domain faster.

Table 2, lists the *DE* as well as the time that the last particle leaves the solution domain. As shown, the time for 5 nm particles is less than the other studied particle diameters. Furthermore, 5 nm particles are more deposited on the walls. Note that at the time history analysis, particle deposition efficiency is calculated by the ratio of deposited particles and the total number of injected particles.

Table 2. Mesh independency analysis for 10 nm particles in a pipe with a diameter of 4.5 mm and length of 6 cm

Particle diameter (nm)	Deposition efficiency (%)	Time (s)
5	17.53	0.31
10	11.11	0.415
20	7.14	0.66
40	4.68	0.985
100	2.65	1.745

Fig. 15 shows the number of escaped particles from the pipe at each moment for different particle diameters. As shown, for all the studied diameters, the maximum number of escaped particles occurred at 0.035 s after the injection. This

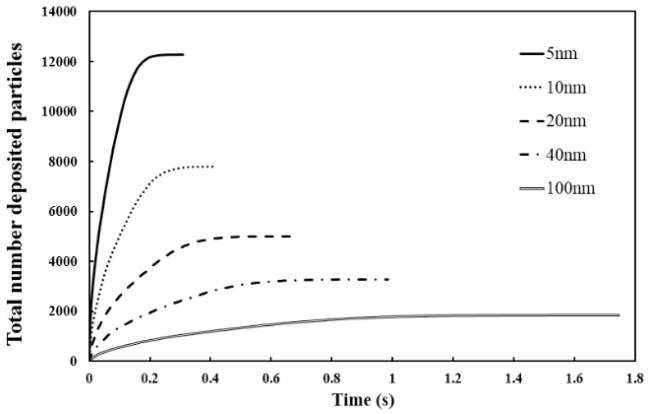

(a)

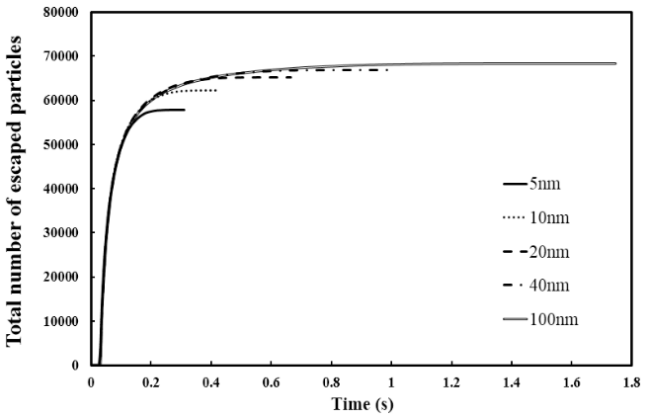

(b)

Fig. 14. The variation of the total number of (a) deposited and (b) escaped particles through the time for different diameters of nano particles

is an important issue that helps improve the deposition at the moment of maximum escaped particles. The reason is due to the inlet velocity and length of the pipe. Since the inlet velocity is 1 m/s, the maximum velocity in the pipe is 2 m/s and due to the length of the pipe equal to 6 cm, the time that maximum number of the particles escape from the domain occurred after the first time step which is equal to 0.035 s [31].

4- Conclusion

The aim of this paper was to study the transport of nano particles in a gas-solid two-phase flow in tubular pipes using the Eulerian-Lagrangian method. After the code verification, the effects of all parameters on the deposition efficiency are studied. In the time history analysis, the effect of particle diameter on the particles deposition and the time duration of escaped particles from the pipe is studied. The following results are achieved in this study:

- *DE* decreases by increasing the pipe diameter, decreasing the pipe length and increasing the inlet velocity.
- Increasing the temperature increases the deposition of nano particles. However, particle density has no effect on *DE*.
- Decreasing the particle diameter causes an increase on deposited particles and also a decrease in the time duration of escaped particles from the domain.
- The maximum number of escaped particles happened at 0.035 s after the injection.

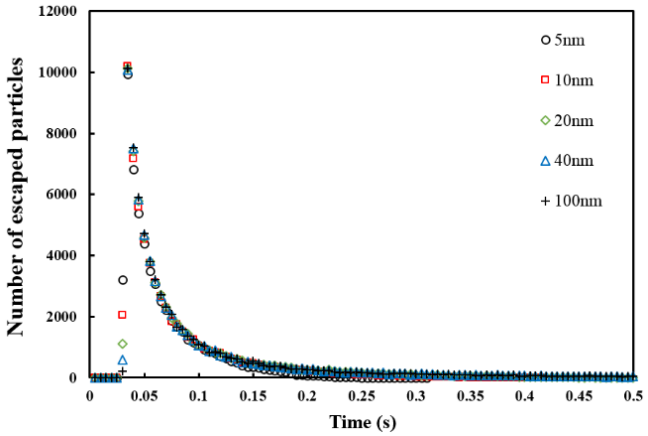

Fig. 15. The variation of number of escaped particles at each moment for different dimaters of nano particles

The results of this paper help in better understanding of the deposition of particles in pipes and also finding new ways to increase the deposition of particles in after treatment systems especially for diesel engines.

Acknowledgements

The authors gratefully acknowledge Prof. Zoran Ristovski from the Queensland University of Technology and Dr. Meisam Babaei from Salford University for their helpful support.

References

[1] C. Marchioli, A. Giusti, M.V. Salvetti, A. Soldati, Direct Numerical Simulation of Particle Wall Transfer and Deposition in Upward Turbulent Pipe Flow, *International journal of Multiphase flow*, 29(6) (2003) 1017-1038.

[2] L. Tian, G. Ahmadi, Particle Deposition in Turbulent Duct Flows - Comparisons of Different Model Predictions, *Journal of Aerosol Science*, 38(4) (2007) 377-397.

[3] J. Tu, K. Inthavong, G. Ahmadi, Computational Fluid and Particle Dynamics in the Human Respiratory System, *Springer Netherlands*, 2012.

[4] V. Golkarfard, P. Talebizadeh, Numerical Comparison of Airborne Particles Deposition and Dispersion in Radiator and Floor Heating Systems, *Advanced Powder Technology*, 25(1) (2014) 389-397.

[5] D.B. Ingham, Diffusion of aerosols from a stream flowing through a cylindrical tube, *Journal of Aerosol Science*, 6(2) (1975) 125-132.

[6] B.S. Cohen, B. Asgharian, Deposition of Ultrafine Particles in the Upper Airways: An Empirical Analysis, *Journal of Aerosol Science*, 21(6) (1990) 789-797.

[7] J.W. Thomas, Assessment of airborne radioactivity, in, Int. *Atomic Energy Agency*,Vienna, 1967, pp. 701-712.

[8] D.B. Ingham, Simultaneous diffusion and sedimentation of aerosol particles in rectangular tubes, *Journal of Aerosol Science*, 7(5) (1976) 373-380.

[9] D.B. Ingham, Diffusion of aerosols in the entrance region of a smooth cylindrical pipe, *Journal of Aerosol Science*, 22(3) (1991) 253-257.

[10] H.C. Yeh, G.M. Schum, Models of human lung airways

and their application to inhaled particle deposition, *Bull Math Biol*, 42 (1980) 461-480.

[11] A. Li, G. Ahmadi, Dispersion and Deposition of Spherical Particles from Point Sources in a Turbulent Channel Flow, *Aerosol Science Technology*, 16 (1992) 209-226.

[12] A. Li, G. Ahmadi, Computer simulation of deposition of aerosols in a turbulent channel flow with rough wall, *Aerosol Science Technology*, 18 (1993) 11-24.

[13] H. Ounis, G. Ahmadi, J.B. McLaughlin, Brownian particles deposition in a directly simulated turbulent channel flow, *Physics of Fluids A*, 5 (1993) 1427-1432.

[14] P. Zamankhan, G. Ahmadi, Z. Wang, P.K. Hopke, Y.-S. Cheng, W.C. Su, D. Leonard, Airflow and Deposition of Nano-Particles in a Human Nasal Cavity, *Aerosol Science and Technology*, 40(6) (2006) 463-476.

[15] K. Inthavong, K. Zhang, J. Tu, Modeling Submicron and Micron Particle Deposition in a Human Nasal Cavity, in: Seventh International Conference on CFD in the Minerals and Process Industries, *CSIRO*, Melbourne, Australia, 2009.

[16] P.W. Longest, S. Vinchurkar, Effects of Mesh Style and Grid Convergence on Particle Deposition in Bifurcating Airway Models with Comparisons to Experimental Data, *Medical Engineering & Physics*, 29(3) (2007) 350-366.

[17] F. Krause, A. Wenk, C. Lacor, W.G. Kreyling, W. Möller, S. Verbanck, Numerical and experimental study on the deposition of nanoparticles in an extrathoracic oral airway model, *Journal of Aerosol Science*, 57 (2013) 131-143.

[18] H. Shi, C. Kleinstreuer, Z. Zhang, C.S. Kim, Nanoparticle transport and deposition in bifurcating tubes with different inlet conditions, *Physics of Fluids*, 16(7) (2004) 2199-2213.

[19] Z. Yin, Z. Dai, Investigating the Nanoparticles Penetration Efficiency through Horizontal Tubes Using an Experimental Approach, *Advances in Mathematical Physics*, (2015).

[20] A. Guha, Transport and Deposition of Particles in Turbulent and Laminar Flow, *Annual Review of Fluid Mechanics*, 40(1) (2008) 311-341.

[21] Z. Zhang, C. Kleinstreuer, C. Kim, Airflow and Nanoparticle Deposition in a 16-Generation Tracheobronchial Airway Model, *Ann Biomed Eng*, 36(12) (2008) 2095-2110.

[22] Q. Ge, K. Inthavong, J. Tu, Local Deposition Fractions of Ultrafine Particles in a Human Nasal-Sinus Cavity CFD Model, *Inhalation Toxicology*, 24(8) (2012) 492-505.

[23] M. Abarham, P. Zamankhan, J.W. Hoard, D. Styles, C.S. Sluder, J.M. Storey, M.J. Lance, D. Assanis, CFD analysis of particle transport in axi-symmetric tube flows under the influence of thermophoretic force, *International Journal of Heat and Mass Transfer*, 61 (2013) 94-105.

[24] J.-Z. Lin, Z.-Q. Yin, P.-F. Lin, M.-Z. Yu, X.-K. Ku, Distribution and penetration efficiency of nanoparticles between 8–550nm in pipe bends under laminar and turbulent flow conditions, *International Journal of Heat and Mass Transfer*, 85 (2015) 61-70.

[25] Y. Shang, J. Dong, K. Inthavong, J. Tu, Comparative numerical modeling of inhaled micron-sized particle deposition in human and rat nasal cavities, *Inhalation Toxicology*, (2015) 1-12.

[26] M. Yousefi, K. Inthavong, J. Tu, Microparticle Transport and Deposition in the Human Oral Airway: Toward the Smart Spacer, *Aerosol Science and Technology*, 49(11) (2015) 1109-1120.

[27] W.C. Hinds, *Aerosol Technology: Properties, Behavior, and Measurement of Airborne Particles*, Wiley, 2012.

[28] K. Inthavong, K. Zhang, J. Tu, Numerical Modelling of Nanoparticle Deposition in the Nasal Cavity and the Tracheobronchial Airway, *Computer Methods in Biomechanics and Biomedical Engineering*, 14(7) (2011) 633-643.

[29] [29] P.W. Longest, J. Xi, Computational Investigation of Particle Inertia Effects on Submicron Aerosol Deposition in the Respiratory Tract, *Journal of Aerosol Science*, 38(1) (2007) 111-130.

[30] P.G. Gormley, M. Kennedy, *Diffusion from a Stream Flowing through a Cylindrical Tube, Proceedings of the Royal Irish Academy*. Section A: Mathematical and Physical Sciences, 52 (1948) 163-169.

[31] P. Talebizadeh, H. Rahimzadeh, G. Ahmadi, R. Brown, K. Inthavong, 2016. "Time history of diesel particle deposition in cylindrical dielectric barrier discharge reactors". *Journal of Nanoparticle Research*, 18:378.

Please cite this article using:

P. Talebizadeh, H. Rahimzadeh, G. Ahmadi, R. Brown, K. Inthavong, "Numerical Investigation of Nano Particles Dispersion and Deposition in Fully Developed Laminar Pipe Flows", *AUT J. Mech. Eng.*, 1(1) (2017) 13-20.

DOI: 10.22060/mej.2016.762